RESEARCH ARTICLE

Hum and Otoacoustic Emissions May Arise Out of the Same Mechanisms

Franz G. Frosch

Private Initiative Brummton, Bad Dürkheim, Germany
frosch.com@t-online.de

Submitted 5/26/2013, Accepted 9/8/2013, Published 1/31/2014

Abstract—Hum, a low-frequency subjective tone, affects approximately 2% of the population. Spontaneous otoacoustic emissions are sounds emitted from the inner ear, which in some cases are also perceived as tinnitus. The mechanisms of their generation, however, are still not well understood. In this paper, it is demonstrated that many properties reported by hum-sufferers (derived from both questionnaires and my own measurements) are also found in spontaneous otoacoustic emissions. The similarities of such responses suggest that both phenomena may be formed by the same mechanism. A hearing model is proposed that overcomes the limitations of the current models and explains the occurrences of spontaneous otoacoustic emissions and hum.

Keywords: Hum—otoacoustic emission—Van der Pol-oscillator—hearing model—tinnitus

Introduction

Hum is most frequently described as sounding like the bass frequency of a diesel engine idling in the distance. Hum is a worldwide phenomenon, also known as "the Hum," "Taos hum," or "Kokomo hum," and according to Mullins and Kelly (1995) it affects approximately 2% of the population (called hearers) with an annoying low-frequency tone. Although many hum sufferers are convinced that their hum derives from an acoustic source, this source typically cannot be identified in the environment (Deming 2004). Everything that is heard without an external sound-equivalent is tinnitus by definition. Tinnitus is usually high-pitched, of central origin, and associated with hearing loss. It does not form beats with neighboring external sounds, does not discontinue for two to three days after long air travel, and does not stop during head rotations. The characteristics of tinnitus come from an analysis of numerous standard questionnaires answered by tinnitus patients (e.g., Stouffer & Tyler 1990). The tinnitus of hum is perceived differently, a fact mostly unknown to otologists. In a questionnaire customized for hearers (Frosch 2008), 60% of hum-sufferers perceive a sound-interactive hum (SIH) that may form beats with, lock into, and match the frequency of an external sound. A time lag of two to three days until hum reappears after longer air travel has been reported by 55% of hearers in the questionnaire, and 37% of hearers report that they can stop their hum during purposeful head movements.

The evidence that hum does not derive from an acoustic source was supplied by eight hum-suffering musicians when they matched their hum with a sound generator at the same place and time to completely different hum-frequencies (Mullins & Kelly 1995). If the musicians perceived hum as a real external sound, they would have all matched to the same frequency, so clearly hum is not an audible external sound. Results were confirmed in 2003 by the IGZAB eV, the "Interest group for Research of the Hum Nuisance" in Bad Waldsee, Germany. The evidence that hum does not derive from any external electromagnetic source, which hum-sufferers sometimes assume next after discounting an external sound-source for their hum, was supplied in 2006, when IGZAB eV board member and researcher Franz G. Frosch reported that hum is perceived unchanged in two validated locales. The first of those locales is a custom shielded chamber in Bad Dürkheim consisting of electrolyte-copper sheets of 1 × 1 × 2 × 0.001 m. The second locale is a magnetically shielded chamber, specifically the BMSR2 chamber of the Physikalisch Technische Bundesanstalt in Berlin, with a shielding factor of more than 10^6 for frequencies of 0.01 Hz and upward. Hearers determined no difference in the hum-perception when stationed either inside or outside of these locales, therefore an instantaneous external electromagnetic cause for hum does not exist.

Spontaneous otoacoustic emissions (SOAEs) are sounds emitted from the inner ear, and these sounds may be measured via sensitive miniature microphones in the ear canal. SOAEs were first recognized by Kemp in 1978 and have proven to be a fascinating field of auditory research since then. SOAEs are a worldwide phenomenon and can be detected in approximately 50% of the population. In most cases subjects are not aware of their SOAEs; however, in some cases they become audible to the subjects as an incidence of annoying tinnitus (Penner 1988). Many lines of evidence support the hypothesis that SOAEs are produced by spontaneous mechanical oscillations within the cochlea, and perhaps by motile properties of the outer hair cells (OHCs). The mechanisms of SOAEs' formation, however, are still difficult to explain.

This study offers methods by which sound interactions can be used to determine the frequency, volume, and linear growth rate of an SIH-oscillator. It supplies an application of these methods by employing a case study. The results, combined with information from questionnaires on hum, are compared with literature results on SOAEs to demonstrate similarities between the phenomena of hum and SOAEs. By integrating the inner ear's vestibule into the hearing process, the properties of hum and SOAEs can be explained.

Investigations on Hum

If not stated differently, the measurements are carried out by the author on his own hum in his right ear, and statistical information from hum-sufferers is derived from the above-mentioned specially designed questionnaires for hearers. According to the information from the questionnaires, the author's experience of hum is representative of the majority of hearers. Otologists consider them to have healthy ears with normal to above-average hearing functions. The author's hum appears as a continuous tone in the middle of the head and exhibits the characteristics of a hum, which is influenced by sounds, head rotations, and long air travels.

Slope (k), intercept (d), and Pearson's coefficient of determination (R^2) of all measurement results that follow the equation $y = kx + d$ are obtained with a least-squares linear regression analysis.

Sound Generation

Acoustic stimuli are delivered via a Sennheiser HD 580 stereo headphone. The headphone is calibrated with an artificial ear type 4153, Brüel & Kjær. It responds between 50 Hz and 200 Hz in an almost flat frequency course, which follows

$$EL_{\mathrm{dB}} = 42 + 20\log(0.35EL_n) \quad (1)$$

EL_n denotes the sinusoidal voltage at the headphone, measured in millivolt peak to peak (mVpkpk), to produce an external sound (*ES*) at a frequency (EF_n) in Hz with a sound pressure level (EL_{dB}) in dB SPL, re 20 μPa.

All instruments and cables are shielded. At the beginning, during, and at the end of each experiment, frequencies, levels, or phases of acoustic sounds are calibrated, measured, or controlled with a digital two-channel oscilloscope Tekscope THS720 from Tektronix, including software designed for this type of oscilloscope to store and analyze data in a computer. Stimuli are produced with customary digital wave generator software in a personal computer, connected to the headphone via a custom-built switch with on/off and ear side change functions, and a cascade attenuator with 12 damping steps from −5 to −80 dB. The oscilloscope is connected parallel to the headphone. Data are read out and notated, then transmitted from the oscilloscope to a second computer for storage and further analysis. The wave generator software enables the installation and management of one or more wave generators at the same time. Each wave generator appears individually on the screen of the computer and can generate signals between 0.2 Hz and 22,050 Hz in 1 kHz, 10 Hz, and 0.1 Hz steps.

Sound Interactions

Hearing Levels (HLs)

To measure the hearing levels, the volume of an external sound is adjusted to the level at which the first audible difference in the hearing impression is noticed. For better signal-discrimination, the external sound is switched on/off occasionally. The hearing levels, shown in Figure 1, are measured during a time period of two to three days, when hum is not audible after more than 4 hours of air travel.

The time lag until hum reappears can sometimes be shorter or longer and can also occur after travelling by other types of transportation. Undoubtedly, only some unusual additional external influences may cause this strange effect. It probably has the same basic cause as the phenomenon of hum-

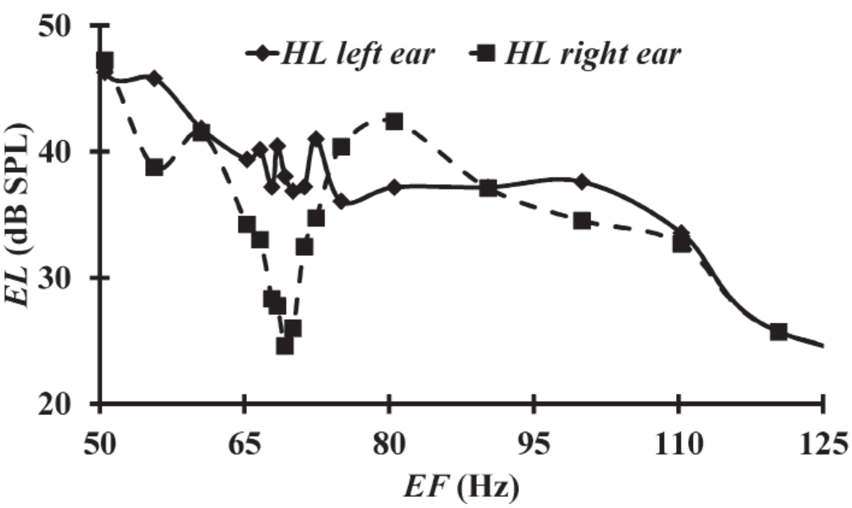

Figure 1. The hearing levels (*HL*s) of both ears are measured from 50 Hz to 125 Hz within 2 d after overseas air travel, when hum is not audible. They are performed with an external sound at frequencies *EF*s and volumes *EL*s. The right ear shows a dip in hearing level at 69 Hz, the hum frequency before air travel and again 2 d after. The hearing level of the left ear shows no dip.

sufferers not hearing their hum at certain locations and periods. Possible causes are exposure to abrupt changes of atmospheric pressure or of the gravity of earth, or to prolonged vibration and noise, all of which are known to affect the vestibule. During this lag time, the right ear can be treated as a band-pass filter with a quality factor Q_3 of 35 that filters external sounds or noise around the hum-frequency selectively to a sound-impression of hum.

Beat Frequencies (BFs)

A fixed number of consecutive beats is stopped with a calibrated customary electronic time clock with a manual start/stop function and a 7-digit display for hour, minute, second, and 1/100 second units.

The beat frequency is calculated by the use of Equation (2):

$$BF = \frac{\text{number of beats}}{\text{time in seconds}} \quad (2)$$

The typical audible interactions between an SIH and a monaurally presented external sound are illustrated in Figure 2. Note that below the hearing

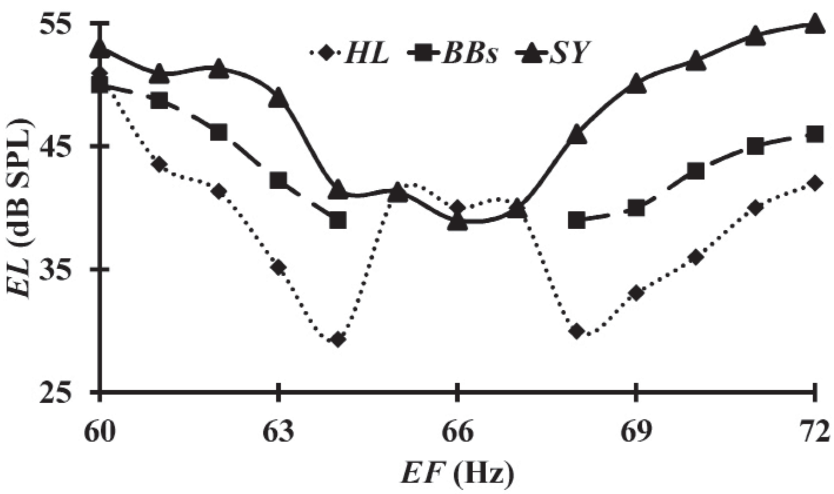

Figure 2. The interactions of hum with external sounds in the right ear, measured at external frequencies (*EF*s) from 60 Hz to 72 Hz in 1-Hz steps by adjusting the external volume (*EL*) to the appropriate volumes to get the hearing level (*HL*), best beats (*BB*s), and synchronization (*SY*). The measurements are typical and performed in one day, when the hum frequency (*HF*) is 66.0 Hz.

level, only hum is heard, and above the synchronization, only the external signal can be heard. Synchronization takes place when hum is locked into the external sound. In between both levels, beats are audible and optimally modulated along the lines of best beats (*BB*s); the beat frequencies increase almost linearly with the distance to the hum frequency (*HF*). At approximately $|EF - HF|$<1 Hz no more beats are formed, and the hearing level merges with the synchronization. The hearing level curve next to the hum frequency corresponds to the synchronization and loudness match of the SIH into the external sound.

The right ear shows a remarkable dip in the hearing level around the hum frequency, which allows measurements in a broad interacting region between the hearing levels and synchronizations. This is not replicated in the left ear, where only poor modulation depths are possible before the SIH synchronizes. This situation becomes obvious when the hearing level-measurements are not falsified by the interaction with an SIH (Figure 1).

The sound interactions make it possible to measure the frequencies and volumes of hum and to simulate the Van der Pol (VDP)-oscillation.

Van der Pol (VDP)-Oscillation

Principles

The VDP-oscillator is a simple model widely used to simulate non-linear biological oscillations because it closely imitates many biological phenomena. The simple harmonic oscillator is generalized by adding a non-linear damping which is negative for small amplitudes, modeling instability, and feeding energy, and which becomes positive for large amplitudes. Because energy is fed into the oscillator, spontaneous sustained oscillation occurs even without periodic driving. The Van der Pol-oscillator has been used successfully to simulate SOAEs, which is an important proof that a nonlinear system drives the SOAE-oscillation. Formulas developed for the application in SOAEs are not suitable for measuring psychoacoustic sound-interactions of hum. In this manuscript, formulas are developed and applied to examine whether an SIH-oscillator can be treated as a VDP-oscillator. Several formulas applicable to psychoacoustic measurements on SIHs are worked out.

Basic Approaches

The equation of the forced VDP-oscillator

$$\frac{d^2n}{dt^2} - \left(\alpha - \beta n^2\right)\frac{dn}{dt} + \omega_0{}^2 n = A\omega_0{}^2 \cos\left(\omega_1 t\right), \qquad (3)$$

as given by Gyergyek, Čerček, and Stanojević (1997) in their equation 1 and applied for an SIH-oscillator has n as the oscillating hum parameter, A as the effective external force amplitude of the sinusoidal sound at the oscillator, $\omega_0 = 2\pi HF$ as the angular frequency with HF as the frequency of the unperturbed (natural frequency) of the hum oscillator in Hz, $\omega_1 = 2\pi EF$ as the angular frequency with EF as the frequency of the external sound in Hz, α as the linear growth rate, and β as the nonlinear damping coefficient.

Appleton (1922) proposes a solution for the VDP-equation by splitting the oscillation into an internal oscillation term a and external oscillation term b. Gyergyek, Čerček, and Stanojević (1997) follow this concept and introduce a new quantity, a_0, in their equation 9,

$$a_0{}^2 = a^2 + b^2 = \frac{2\alpha}{\beta}, \tag{4}$$

which relates to the amplitude of the unperturbed VDP-oscillator. In their equation 10, they formulate a relation between a, b, ω, and A, (our study neglects a, because it is very small or zero) to get

$$b^2\left[\left(\frac{\omega_0{}^2 - \omega_1{}^2}{\omega_0{}^2}\right)^2 + \frac{\alpha^2\omega_1{}^2}{\omega_0{}^4}\left(1 - \frac{b^2}{a_0{}^2}\right)^2\right] = A^2 \tag{5}$$

as a suitable equation to find solutions for the SIH-interactions synchronizations, best beats, loudness matches, and periodic pulling between hum and an external sound to determine the hum frequency and volume as well as to simulate the VDP-oscillation.

Synchronizations (SYs)

The phenomenon of synchronization can also be described in the terms *phase locking* or *frequency entrainment*. This phenomenon can be simulated with an external sound, swept at a fixed volume toward the SIH-frequency until beats just come to a stop. As a result, the hum-oscillation is suppressed completely by the external sound, $a = 0$, and Equation (4) changes into $b^2 = a_0{}^2$. Using this boundary condition and the approximation $HF + EF_1 = 2HF$, Equation (5) results in

$$EL_1 = 2\left(HF - EF_1\right)\frac{1}{HF}\frac{a_0}{\mathrm{T}_1} \tag{6}$$

or

$$EF_2 - EF_1 = HF \frac{T_1}{a_0} EL_1. \tag{7}$$

EF_1 and EF_2 are the lower and upper frequencies of the synchronization-boundaries of an external sound at the volume EL_1. The other parameters are the hum frequency (*HF*), the signal-strength of the hum-oscillator a_0, and the signal transfer factor T_1. T_1 corrects the change of the external force amplitude from the earphone EL_n to the hum-oscillator A_n:

$$EL_n T_1 = A_n. \tag{8}$$

The approximation $HF + EF_1 = 2HF$ seems justified because the hum frequency and external frequency are usually 1 Hz to 3 Hz apart and never exceed a difference of more than 5 Hz, so that $HF + EF \approx 2HF \approx 2EF$.

A diagram with $EF_2 - EF_1$ as ordinate, EL_1 as abscissa, according to Equation (7) has the slope *S*

$$S = HF \frac{T_1}{a_0}, \tag{9}$$

and rearranged is

$$\frac{a_0}{T_1} = \frac{HF}{S}. \tag{10}$$

Equation (10) allows the calculation of a_0/T_1, which represents the signal-strength of the hum-oscillation, calculated as external sound travelling to the hum-oscillator. A typical synchronization chart with the upper and lower frequency boundaries EF_2 and EF_1 of the synchronization region dependent on the external volume is shown in Figure 3. The same data, plotted as shown in Figure 4, calculates the slope *S* of Equation (7). The hum frequency is measured before and after each experiment and represents the data at $EL = 0$. Equation (10) is used to calculate a_0/T_1.

Results: *hum frequency*: 67.16 Hz, 0.72, 10; *S*: 0.96 Hz/mVpkpk, 0.117, 10; R^2: 0.97, 0.018, 10; a_0/T_1: 70.96 mVpkpk, 8.90, 10. (*Measure*: mean, standard deviation, number of measurements, etc.)

Best Beats (BBs)

Best beats between an external sound and an SIH sound like beats between two equally loud external sounds. At the appropriate external volume, the

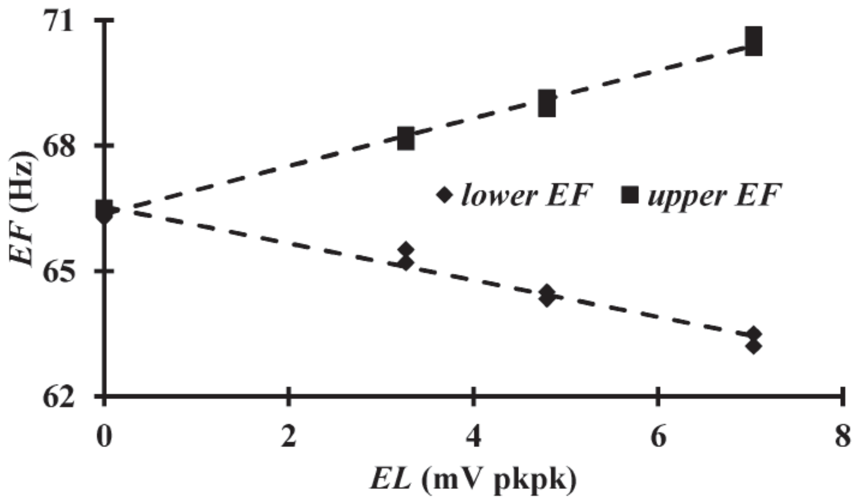

Figure 3. The synchronization-course of the hum in the right ear with external sounds is measured at three different volumes (*EL*s) between 3 and 7 mVpkpk by spreading the frequency for each volume into the boundary of the upper and lower frequency (*EF*) until synchronization appears. It is a typical measurement of one day at a hum-frequency of 66.3 Hz. The external frequency at the external volume *EL* = 0 corresponds to the hum frequency of that day.

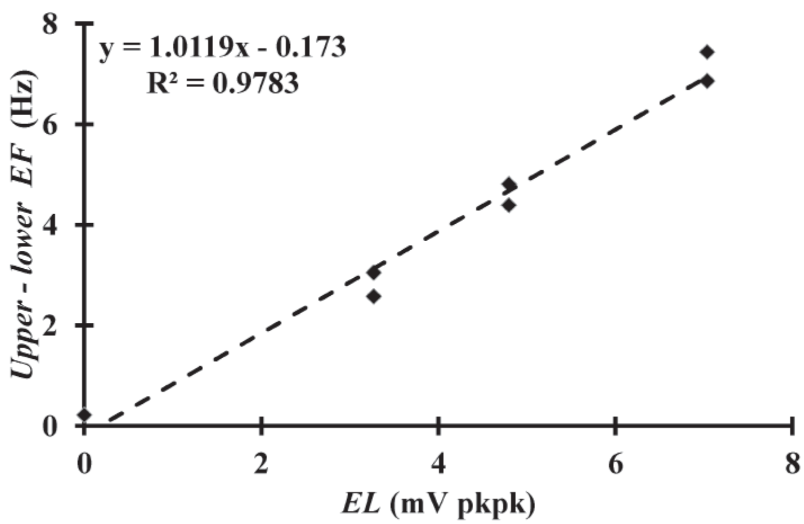

Figure 4. The synchronization-course of the hum with the same data as in Figure 3; however, the differences of the upper and lower external frequencies (EF_2–EF_1) as a function of their external volumes (*EL*) are plotted. The slope of the line corresponds to $HF\ T_1/a_0$ in Equation (7).

internal and external oscillation terms of the VDP-oscillator are equal ($a = b$), and Equation (4) changes into

$$b^2 = \frac{a_0^{\ 2}}{2}. \tag{11}$$

Using the boundary conditions of Equation (11), the approximations $HF + EF = 2HF$, and $EF^2 / HF^4 = 1 / HF^2$, Equation (5) changes into

$$EL_2 = \frac{a_0}{\mathrm{T}_1}\frac{1.41}{HF}\sqrt{\left(HF - EF_1\right)^2 + 0.00158\alpha^2}. \tag{12}$$

EL_2 denotes the volume of an external sound necessary to get best beat-interactions at the external frequency (EF_1). Synchronization- and best beat-curves cross each other when EL_1 of Equation (6) and EL_2 of Equation (12) are equal. At the crossing points, the distance between the upper and lower frequency is

$$EF_2 - EF_1 = 0.080\alpha \tag{13}$$

and the corresponding sound intensity is

$$EL_1 = EL_2 = 0.080\frac{\alpha}{HF}\frac{a_0}{\mathrm{T}_1}. \tag{14}$$

An external sound can no longer generate best beats with an SIH at frequencies between the two crossing points. Best beats can be formed easily in the right ear as shown in Figure 2, but, significantly, not in the left. Nevertheless, it is possible to determine SIH-frequencies in both ears.

Loudness Matches

At the loudness match, the external sound is adjusted to the SIH in frequency and volume until they cannot be differentiated from each other. The frequency differences disappear, $EF = HF$, and Equation (12) reduces to

$$EL_3 = 0.056\frac{\alpha}{HF}\frac{a_0}{\mathrm{T}_1}. \tag{15}$$

EL_3 is the volume of an external sound, which is necessary to match the loudness of the SIH-oscillator and in terms of figures to generate *BB*s at

EF – *HF* = *BF* = 0. At the beginning of each loudness-match experiment, the hum frequency is determined and the external sound is adjusted to this frequency. Then the external volume is increased stepwise, until it is noticeable as being just louder than the unperturbed hum. For better signal-discrimination, the external sound is switched on/off occasionally. The data are analyzed according to Equation (15).

Results: *hum frequency* (*HF*): 66.23 Hz, 0.85, 10; *volume loudness match* (EL_3): 1.61 mVpkpk, 0.40, 10; a_0/T_1: 66.43 mVpkpk, 16.39, 10, using Equation (15), and $\alpha = 34.35\ s^{-1}$ from the periodic pulling.

The volume EL_3 necessary for loudness match is identical to the volume of the unperturbed SIH-oscillation a_0, which, according to Equation (15), also depends on the hum frequency, the linear growth rate, and the transmission factor.

Hum Frequency (HF)

The frequency of an external sound (*EF*) is adjusted approximately 3 Hz above or below the hum frequency to a volume necessary to receive best beats with the SIH-oscillator. The time needed for 100 consecutive beats is stopped; the beat frequency (*BF*) is calculated with Equation (2), and the hum frequency with Equation (16).

$$HF = EF \pm BF \tag{16}$$

In the right ear, a series of 40 consecutive measures of the hum frequency, according to Equation (2) and Equation (16), has approximately normal distribution with a standard deviation of 0.145%, or 0.10 Hz. The fluctuation can be attributed to the short-time frequency-fluctuation of the SIH-oscillator because, in comparison, a series of 40 consecutive measures of two external sounds of 147 Hz and 150 Hz having 3 Hz difference and equal volumes generates normally distributed beat frequencies at a standard deviation of 0.002%, or 0.003 Hz, when related to the external sound of 150 Hz, which corresponds to the accuracy of this method.

The frequency of the SIH in the right ear drifts over 10 years at a rate of −0.44 Hz/year from 70 Hz to 66 Hz. For the left ear, the generation of best beats is not possible. Beats occur, though not optimally modulated, in a small range of the external sound only. Oscillations around 58 Hz are assumed to occur in the left ear.

Hum Volume

a_0/T_1 describes the volume of the hum-oscillation received by the interactions of external sounds with the hum-oscillator using formulas used for the Van der Pol-oscillator. The volume of a conceivable SOAE, possibly induced by the hum-oscillation, can be estimated thereof. On the assumptions that $EL_3 = a_0$ and inward and outward transmissions are identical at $T_1 = T_{-1} = 0.03$, a SOAE would have a volume of 9 dB SPL; hence, it would be deeply embedded in the body's natural microvibration (Rohracher 1962).

Periodic Pulling

Periodic pulling describes the pulling of the frequency of an SIH toward the external frequency (*EF*). At frequency differences smaller than 2 Hz, the hum frequency (*HF*) is pulled significantly toward the external frequency. The beat frequency (*BF*) then becomes smaller than $|EF - HF|$. The formula

$$2\pi BF = \left(|\omega_1 - \omega_0|\right)\sqrt{1 - \frac{\alpha^2}{16(\omega_0 - \omega_1)^2}}, \tag{17}$$

as given by Gyergyek, Čerček, and Stanojević (1997) in their equation 30, squared and rewritten, results in

$$BF^2 = (EF - HF)^2 - \frac{\alpha^2}{64\pi^2}. \tag{18}$$

A diagram with $(BF)^2$ as ordinate and $(EF-HF)^2$ as abscissa has the y-intercept d as

$$d = -\frac{\alpha^2}{64\pi^2}, \tag{19}$$

and rearranged is

$$\alpha = 25\sqrt{-d}. \tag{20}$$

Equation (20) allows the calculation of the linear growth rate α.

To measure the periodic pulling, the frequency of an external sound is changed stepwise toward the direction of the hum frequency while keeping the volume constant. The beat frequency is measured between each step. This action is performed at a series of different volumes. The resulting data are analyzed according to Equation (18) and Equation (20). Figure 5 shows the relation between the beat frequency and external frequency of one typical dataset. The same data plotted using Equation (18), as shown in Figure 6, has the y-intercept *d*, which allows the calculation of *α* with Equation (20). The hum frequency is measured before and after each experiment.

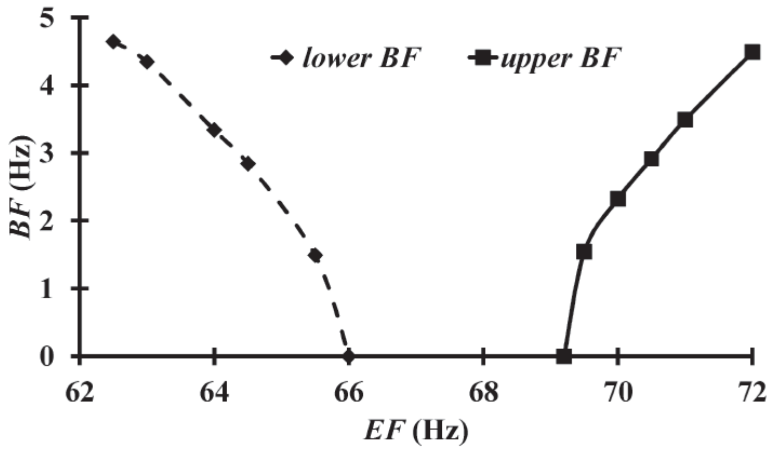

Figure 5. A typical periodic pulling is measured in one day, when the hum frequency is at 67.5 Hz. At a constant external volume of 3.3 mVpkpk, the beat frequency (*BF*) is measured for different external frequencies (*EF*s).

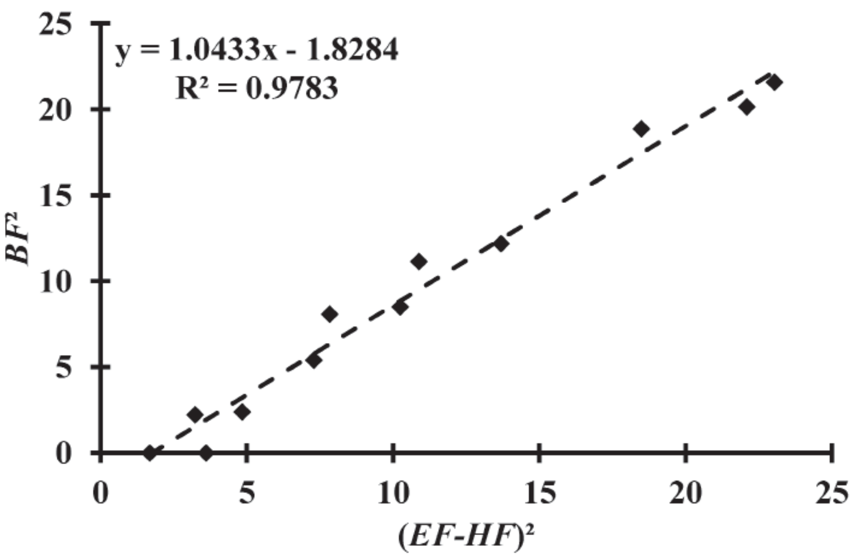

Figure 6. The measurements of the periodic pulling with the same data as in Figure 5; however, BF^2 against $(EF - HF)^2$ to get *α* from the y-intercept according to Equation (20) is plotted.

Results: *hum frequency*: 66.65 Hz, 0.853, 10; $-d$: 2.09 s^{-2}, 1.041, 10, R^2: 0.98, 0.025, 10; α: 34.35 s^{-1}, 8.455, 10.

Simulating the Van der Pol (VDP)-Oscillator

The values for a_0/T_1, obtained by loudness match in combination with periodic pulling, are not statistically different at a significant level ($p < 0.01$) when compared with the values obtained from synchronization-measurements. The two sample t-tests with equal sample size and unequal variance results in $t_{calc} = 0.768 < t_{table} = 2.878$. It is concluded that the sound-interactions of an SIH follow the rules of a forced VDP-oscillator.

The courses of the synchronizations and the best beats follow Equation (6) and Equation (12). By use of a_0/T_1 = 68.7 mVpkpk, *HF* = 66.5 Hz, and α = 34.4 s^{-1}. Figure 7 shows the courses for the best beats and the synchronizations, which partially simulate the measures previously shown in Figure 2.

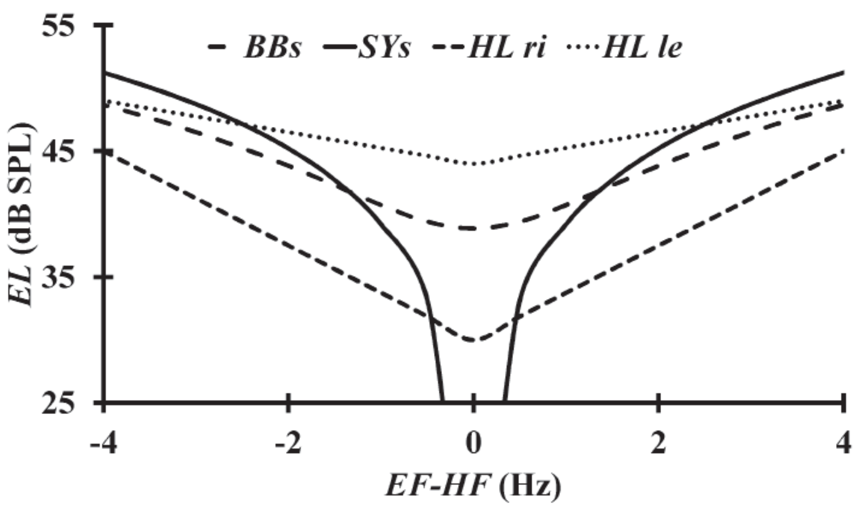

Figure 7. The hum-oscillation is simulated as a forced Van der Pol-oscillation. The hum parameters a_0/T_1 = 68.7 mVpkpk, α = 34.4 s^{-1} received for the right ear, allowing the calculation of the synchronizations (*SY*s) and best beats (*BB*s) with Equation (6) and Equation (12) and simulating the interactions of an external sound at the frequency (*EF*) and the volume (*EL*) with a hum of a frequency (*HF*). The hearing levels (*HL*s) for both ears are added for comparison.

Head Rotations

Active head rotations on the horizontal view-axis are performed over fixed angles; the subject sits in a chair one meter away from a mirror. The head rotates over the neck while the horizontally oriented eyes focus at a mark on the mirror. The angles vary from 2° to 96°, using a variable angle limiter, and movements are controlled in the mirror. Rotations are adjusted to a speed necessary to just discontinue the hum before 10 consecutive head orientations from the limit of one side to the limit of the other are stopped and averaged into one data point. 86 data points are plotted in Figure 8, resulting in an x-intercept of 0.09 s, which is interpreted as the time necessary to reverse the direction, and a slope of 306°/s, interpreted as the average velocity of the rotation needed to stop hum, which is independent of the rotation-angle. Some 37% of hearers in the questionnaire report that they can stop their hum during purposeful head movements. In our study, only horizontal head rotations influenced hum. Hum can also be influenced by minute head rotations, which move the location of the hum impression from the side of the head to the right ear (when rotating to the left) and to the left ear (when rotating to the right) without noticeable changes in

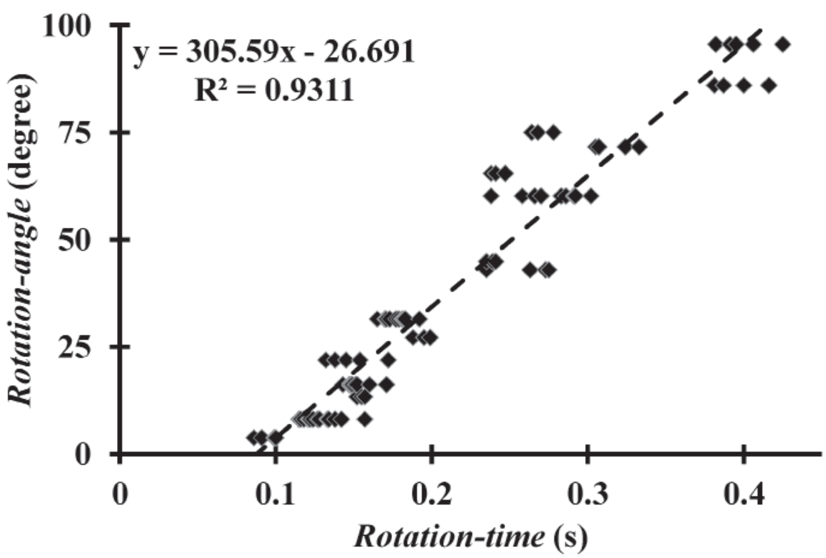

Figure 8. Voluntary head rotations are measured for horizontal rotation angles from 2° to 96°. The slope of the line represents a velocity of 306°/s, which is necessary to just stop hum.

the frequency or volume of the hum. Independent of the rotation direction, hum is removed above an angular velocity of 306°/s. Identical results are found for self-generated head-on body rotations and body rotations over the legs. Fixing one's gaze at a spot during rotation, visually following the rotation, or even closing one's eyes have no influence on the observed hum-influencing effect. This rules out muscle reflexes as the cause. Instead, hum involved acoustic elements present in the semicircular canals in order to influence hum by head rotations.

Hum can be differentiated from an external sound with the pitch of hum by head rotations. During active head rotations above 306°/s, hum is not audible, while the audibility of the external sound remains unchanged.

Similarities between Hum and SOAEs

Many of the same properties that hum-sufferers report via questionnaires, personal information, and the results of measurements described here are also reported for SOAEs. The results are qualitatively identical. For instance, the hum-frequency in the case study decreases at a rate of 0.6%/year, compared with a rate between 0.13%/year and 0.41%/year for SOAEs (Burns 2009). A sound interactive hum (SIH) can be simulated as a Van der Pol (VDP)-oscillator. The linear growth rate α of the oscillation has a value of 35 s^{-1} in our case study, compared with 40–500 s^{-1} found for SOAEs (Murphy, Talmadge, & Tubis 1995). Hum sometimes appears in local dips at the minima of the hearing level, with a high quality factor (Q_3 of 35 for the right ear in Figure 1), which is also found for SOAEs (Dallmayr 1985). Hum interacts with external sounds (as reported by 60% of hearers in the questionnaire) to form the synchronizations and periodic pulling demonstrated here, which is also reported for SOAEs (Schloth & Zwicker 1983, Talmadge, Tubis, Long, & Piskorski 1998). Approximately 2% of the population perceives an annoying hum (Mullins & Kelly 1995), therefore it is likely that SOAEs become audible as frequently and as annoyingly (Penner 1988). In our case study, an annoying hum was removed with a daily aspirin dosage of 2.4 g within the first day (confirmed by other hearers not in the study), which is comparable to the dosage necessary to remove an SOAE (Penner & Coles 1992) and may be comparable to that for monaural diplacusis, as found for the left ear and also reported for SOAEs (Bacon & Viemeister 1985, Long 1998). The sensation of hum may stop during head movements, as reported by 37% of the hearers in the questionnaire. In our study, it stops during horizontal head rotations above a velocity of 306°/s. These effects are comparable to head movements that reduce the volume of SOAEs (de Kleine, Witt, van Dijk, & Avan 2000, Büki et al. 2000).

As the effects observed for hum seem identical to those observed for SOAEs, audible SOAEs may underlie the same type of tinnitus. From these abundant similarities, it follows that because hum has been found to disappear temporarily after long air travel—reappearing after a time-lag of two to three days—the same temporary cessation may also occur for some SOAEs. On the other hand, when using a method tailor-made for hum-detection, the mechanical hum-oscillation also may be detectible objectively. An additional hearing pathway that involves the vestibular system seems necessary to explain these observations on hum and SOAEs.

Discrepancies in Current Hearing Models

Information about the phase relations of sounds cannot be received from the travelling wave, which considerably changes its group delay depending on frequency and/or volume (Serbetcioglu & Parker 1999, Palmer & Shackleton 2008). The arguments that the determination of the exact phase-information is received through the rate–place representations suffer from the fact that the firing rate of the majority of auditory nerve fibers is saturated equally and cannot discriminate the primary frequencies of beats. Auditory nerves do receive accurate rate information (Sachs & Young 1980); therefore, this information must come from another site. Knowledge of the frequency/phase relations is necessary to get information on sound-image and becomes crucial when several sounds interact. Speech recognition falls into this category when formants have to be analyzed (Young & Sachs 1979).

After sectioning the olivocochlear bundle at the floor of the fourth ventricle by cutting the lateral olivocochlear and medial olivocochlear efferent systems, there is no change in the fundamental aspects of the threshold response of cochlear afferents, including the relationship between threshold and spontaneous rates (Liberman 1990). Contrary to the conclusion of Thiers, Nadol, and Liberman in 2008 that the efferent system is not needed for these fundamental aspects, the above observation provides evidence that the vestibular system, including cochlear efferents and possibly consisting of paired afferent and efferent specialization, is indeed the primary route for information because they are not disconnected by the cut.

The cochlear microphonic potential recorded at the round window has not been found to be generated by travelling waves at the cochlear base but instead by the fluid pressures (condensations/rarefactions) induced in the cochlear fluids by sound-induced stapes footplate vibrations in an unknown fashion (Perez, Freeman, Sichel, & Sohmer 2007, He et al. 2012). This technical observation offers further evidence that the vestibular system is involved in the hearing process.

There is a preservation of frequency selectivity in the timing pattern of complex signals in view of saturation of both discharge rate and vector strength at moderate intensities to sinusoidal signals. As most fibers discharge at saturation level, it is difficult to infer the location of spectral prominences on the basis of the spatial pattern of rate activity. Neural synchronization is one means by which spectral information is preserved across a wide range of intensities in the presence of saturating and compressive nonlinearities. However, the physiological basis of frequency selectivity may actually be derived from other properties (Greenberg, Geisler, & Deng 1986).

The scientific consensus of the inner ear functions still strictly separates the vestibular system, consisting of three semicircular canals, the sacculus and utriculus, as being responsible for equilibrium only, and considers the cochlea to be the only system responsible for hearing. OHCs and inner hair cells are considered the primary auditory receptors, which sense sound through deflection of their hair cells, which is initiated by the deformation of the basilar membrane caused by the travelling wave or resonance (Dancer 1992, Ruggero 1994). It is still believed the first processing stage is the cochlea which performs a frequency analysis.

It is easily conceivable that the phase-information of a sound is generally built up by pressure waves arriving at semicircular vestibular hair cells from the oval window; Type II hair cells are found to be especially sensitive to hydrostatic pressure (Fraser, Cruickshank, & Shelmerdine 2003). The cristae ampullaris may function as pressure-to-displacement converters. Canal afferent fibers are capable of responding to stimuli at large frequencies (Highstein, Rabbitt, Holstein, & Boyle 2005).

Proposed Hearing Model

According to the found sensitivity of hum and SOAEs to head rotations, a modified hearing model for the inner ear that integrates the vestibular system into the normal hearing route must be proposed. A plausible solution can be developed as follows: A fast vestibular route is established, including an efferent feedback into the cochlea, to act in the timescale in front of the traditional route of the slower travelling wave. An external sound generates at the oval window longitudinal sound pressure waves into the scala vestibula; from here they spread synchronously from the cochlea to the semicircular canals. The vestibular hair cells then detect the primary time-information of a sound and transmit it in parallel running subsets of information through vestibular afferents into the brain. The brain merges all the subsets into one piece of phase/frequency information, performs a signal correlation with an existing frequency–place map, and sends the resultant phase/place/frequency information through a bulk of cochlear efferents into the allocated location of the cochlea. It is possible that shunts between vestibular afferents and the closely spaced cochlear efferents speed up the transportation of the information via vestibulocochlear anastomosis directly from the vestibular afferents to cochlear efferents into the cochlea (Labrousse et al. 2005). Cristae ampullaris, in addition to their function as pressure-to-displacement converters, may also act as amplifiers supporting the oscillation mechanically or electrically. The traditional hearing route (the cochlear pathway) starts, as usual, at the same time at the oval window with the slower transversal travelling waves along the cochlea from base to apex, the outer and inner hair cells, and the cochlear afferents. With this proposed hearing model, the primary phase-information would be already available at the characteristic frequency of the cochlea through the fast vestibular route when the travelling wave arrives at this place. It sharpens the signal at that place in the cochlea, where the place-invariable phase of a bulk of efferent-influenced oscillating OHCs and the place-variable phase initiated by the travelling wave coincide and superimpose. This process can be easily deduced from observing flat phase changes in the scala vestibula that follow sounds, which would not occur without a phase-presetting activity of cochlear efferents onto a bulk of OHCs (Dancer & Franke 1980).

Chronologically, the information of the primary time-coded phase/ frequency of a sound has to already be available as place-coded phase/ frequency information in the cochlea when the travelling wave arrives at this site. This enables the analysis of formants and the establishment of the exact phase-information as a reference point for all signals contained in the travelling wave of the cochlea. If we were to make an analogy between sounds managed in the ear and an orchestra, the vestibular route (including the backward route into the cochlea) would behave as the conductor and the cochlear route (including the cochlear afferents) as the musicians.

Preconditions for the Generation of SOAEs and Hum

A sound generates in-phase oscillations along the middle ear and the scala vestibula of the cochlea only at limited frequency-ranges. This is the case at approximately 3 kHz (1000–8000 Hz) and less than 150 Hz for guinea pigs (Dancer & Franke 1980), and can be expected for humans at approximately 2 kHz (800–5000 Hz) for SOAEs (Dallmayr 1985), and 30–80 Hz for hum (Mullins & Kelly 1995). Within these frequency-ranges the phases of sound-pressure waves in the scala vestibula are almost identical to the phases in the middle ear and to the cochlear efferent feedback and do not damp each other. Sound-pressure waves generated in the scala vestibula by over-tuned OHCs may induce a feedback mechanism even without an external sound when they involve the semicircular canals and vestibular afferents and are in phase retransmitted by cochlear efferents to the place/frequency site of the oscillating OHCs to support the oscillation and close the circuit. The oscillation may be detectable in the ear canal as SOAE and may generate a travelling wave, influence cochlear afferents at the characteristic frequency, and become audible.

Conclusions

Previous research establishes that hum is not an external sound and has no electromagnetic causes. This paper proposes that hum has the same origin as the more extensively studied SOAEs. Understanding the common origin of these phenomena will help hearers to cope with this annoying condition and encourage manufacturers to develop specially designed maskers.

The phenomena of hum and spontaneous otoacoustic emissions seem to start with an oscillation of a bulk of OHCs supported by a feedback circuit (including the vestibular system) to sharpen and stabilize a self-sustained oscillation, which makes it necessary to modify the current hearing model. Because of the small size of the auditory organs, and because animals cannot tell us what they hear when tested, it will be a long and difficult process to run experiments that determine the detailed functions of the ear and to potentially verify the hearing model of this paper.

References

Appleton, E. V. (1922). The automatic synchronization of triode oscillators. *Proceedings of the Cambridge Philosophical Society*, *21*, 231–248.

Bacon, S. P., & Viemeister, N. F. (1985). A case study of monaural diplacusis. *Hearing Research*, *19*, 49–56.

Büki, B., Chomicki, A., Dordain, M., Lemaire, J. -J., Wit, H. P., Chazal, J., & Avan, P. (2000). Middle-ear influence on otoacoustic emissions. II: Contributions of posture and intracranial pressure. *Hearing Research*, *140*, 202–211.

Burns, E. M. (2009). Long-term stability of spontaneous otoacoustic emissions. *Journal of the Acoustical Society of America*, *125*, 3166–3176.

Dallmayr, C. (1985). Spontane oto-akustische Emissionen: Statistik und Reaktion auf akustische Störtöne ("Spontaneous otoacoustic emissions: Statistics and the reaction to acoustic suppression tones"). *Acustica*, *59*, 67–75.

Dancer, A. (1992). Experimental look at cochlear mechanics. *Audiology*, *31*, 301–312.

Dancer, A., & Franke, R. (1980). Intracochlear sound pressure measurements in guinea pigs. *Hearing Research*, *2*, 191–205.

de Kleine, E., Witt, H. P., van Dijk, P., & Avan, P. (2000). The behavior of spontaneous otoacoustic emissions during and after postural changes. *Journal of the Acoustical Society of America*, *107*, 3308–3316.

Deming, D. (2004). The hum: An anomalous sound heard around the world. *Journal of Scientific Exploration*, *18*, 571–595.

Fraser, P. J., Cruickshank, S. F., & Shelmerdine, R. L. (2003). Hydrostatic pressure effects on vestibular hair cell afferents in fish and crustacean. *Journal of Vestibular Research*, *13*, 235–242.

Frosch, F. (2008). Neue Erkenntnisse zum Brummton (New findings on Hum). *Tinnitus-Forum*, *4*, 42–43.

Greenberg, S, Geisler, C. D., & Deng, L. (1986). Frequency selectivity of single cochlear-nerve fibers based on the temporal response pattern to two-tone signals. *Journal of the Acoustical Society of America*, *79*, 1010–1019.

Gyergyek, T., Čerček, M., & Stanojević, M. (1997). Experimental evidence of periodic pulling in a weakly magnetized discharge plasma column. *Contributions to Plasma Physics*, *37*, 399–416.

He, W., Porsov, E., Kemp, D., Nuttal, A. L., & Ren, T. (2012). The group delay and suppression pattern of the cochlear microphonic potential recorded at the round window. *PLoS ONE 7*(3): e34356, http://www.plosone.org/article/info%3Adoi%2F10.1371%2Fjournal.pone.0034356.

Highstein, S. M., Rabbitt, R. D., Holstein G. R., & Boyle, R. D. (2005). Determinants of spatial and temporal coding by semicircular canal afferents. *Journal of Neurophysiology*, *93*, 2359–2370.

Kemp, D. T. (1978). Stimulated acoustic emission from within the human auditory system. *Journal of the Acoustical Society of America*, *64*, 1386–1391.

Labrousse, M., Leveque, M., Ouedraogo, T., Avisse, C., Chays, A., & Delattre, J. F. (2005). An anatomical study of the vestibulocochlear anastomosis (anastomosis of Oort) in humans: Preliminary results. *Surgical and Radiologic Anatomy*, *27*, 238–242.

Liberman, M. C. (1990). Effects of chronic cochlear de-efferentation on auditory-nerve response. *Hearing Research*, *49*, 209–224.

Long, G. (1998). Perceptual consequences of the interactions between spontaneous otoacoustic emissions and external tones. I. Monaural diplacusis and aftertones. *Hearing Research*, *119*, 49–60.

Mullins, J. H., & Kelly J. P. (1995). The mystery of the Taos hum. *Echoes*, *5*, 1–6.

Murphy, W. J., Talmadge, C. L., & Tubis, A. (1995). Relaxation dynamics of spontaneous otoacoustic emissions perturbed by external tones. I. Response to pulsed single-ton suppressors. *Journal of the Acoustical Society of America*, *97*, 3702–3710.

Palmer, A. R., & Shackleton, T. M. (2008). Variation in the phase of response to low-frequency pure tones in the guinea pig auditory nerve as functions of stimulus level and frequency. *Journal of the Association for Research in Otolaryngology*, *10*, 233–250.

Penner, M. J. (1988). Audible and annoying spontaneous otoacoustic emissions: A case study. *Archives of Otolaryngology—Head and Neck Surgery*, *114*, 150–153.

Penner, M. J., & Coles, R. R. (1992). Indications for aspirin as a palliative for tinnitus caused by SOAEs: a case study. *British Journal of Audiology*, *26*, 91–96.

Perez, R., Freeman, S., Sichel, J. Y., & Sohmer, H. (2007). The cochlear microphonic potential does not reflect the passive basilar membrane travelling wave. *Journal of Basic and Clinical Physiology and Pharmacology*, *18*, 159–172.

Rohracher, H. (1962). Permanente rhythmische Mikrobewegungen des Warmblüter-Organismus ("Mikrovibration") (Permanent rhythmic micro-movements of the warm-blooded organism ("microvibration")). *Naturwissenschaften*, *49*, 145–150.

Ruggero, M. A. (1994). Cochlear delays and travelling waves: Comments on "Experimental look at cochlear mechanics." *Audiology*, *33*, 131–142.

Sachs, M. B., & Young, E. D. (1980). Effects of nonlinearities on speech encoding in the auditory nerve. *Journal of the Acoustical Society of America*, *68*, 858–875.

Schloth, E., & Zwicker, E. (1983). Mechanical and acoustical influences on spontaneous oto-acoustic emissions. *Hearing Research*, *11*, 285–293.

Serbetcioglu, M. B., & Parker, D. J. (1999). Measures of cochlear travelling wave delay in humans: I. Comparison of three techniques in subjects with normal hearing. *Acta oto-laryngologica*, *119*, 537–543.

Stouffer, J. L., & Tyler, R. S. (1990). Characterization of tinnitus by tinnitus patients. *Journal of Speech and Hearing Disorders*, *55*, 439–453.

Talmadge, C. L., Tubis, A., Long, G. R., & Piskorski, P. (1998). Modeling otoacoustic emission and hearing threshold fine structures. *Journal of the Acoustical Society of America*, *104*, 1517–1543.

Thiers, F. A., Nadol Jr., J. B., & Liberman, M. C. (2008). Reciprocal synapses between outer hair cells and their afferent terminals: Evidence for a local neural network in the mammalian cochlea. *Journal of the Association for Research in Otolaryngology*, *9*, 477–489. doi: 10.1007/s10162-008-0135-x. http://www.ncbi.nlm.nih.gov/pubmed/18688678

Young, E. D., & Sachs M. B. (1979). Representation of steady-state vowels in the temporal aspects of the discharge patterns of populations of auditory-nerve fibers. *Journal of the Acoustical Society of America*, *66*, 1381–1403.